Shear-Rate-Independent Diffusion in Granular Flows

Yi Fan,[1,2,*] Paul B. Umbanhowar,[1] Julio M. Ottino,[1,3,4] and Richard M. Lueptow[1,4,†]
[1]Department of Mechanical Engineering, Northwestern University, Evanston, Illinois 60208, USA
[2]The Dow Chemical Company, Midland, Michigan 48667, USA
[3]Department of Chemical and Biological Engineering, Northwestern University, Evanston, Illinois 60208, USA
[4]The Northwestern Institute on Complex Systems (NICO), Northwestern University, Evanston, Illinois 60208, USA
(Received 21 April 2014; published 18 August 2015)

We computationally study the behavior of the diffusion coefficient D in granular flows of monodisperse and bidisperse particles spanning regions of relatively high and low shear rate in open and closed laterally confined heaps. Measurements of D at various flow rates, streamwise positions, and depths collapse onto a single curve when plotted as a function of $\dot{\gamma}\bar{d}^2$, where $\bar{d}$ is the local mean particle diameter and $\dot{\gamma}$ is the local shear rate. When $\dot{\gamma}$ is large, D is proportional to $\dot{\gamma}\bar{d}^2$, as in previous studies. However, for $\dot{\gamma}\bar{d}^2$ below a critical value, D is independent of $\dot{\gamma}\bar{d}^2$. The acceleration due to gravity g and particle stiffness (or, equivalently, the binary collision time t_c) together determine the transition in D between regimes. This suggests that while shear rate and particle size determine diffusion at relatively high shear rates in surface-driven flows, diffusion at low shear rates is an elastic phenomenon with time and length scales dependent on gravity ($\sqrt{\bar{d}/g}$) and particle stiffness ($t_c\sqrt{\bar{d}g}$), respectively.

DOI: 10.1103/PhysRevLett.115.088001 PACS numbers: 45.70.-n, 47.57.Gc, 66.30.-h, 81.05.Rm

Collisional diffusion in granular flow results from the random motion and interaction of flowing particles. Diffusion of effectively athermal particles has important implications in nonequilibrium systems such as granular materials (e.g., mixing [1,2], segregation [3–5], rheology [6]) and colloidal suspensions [7]. For granular materials, particle diffusion varies with the nature of the flow. In gaslike dilute flow where binary particle collisions dominate, kinetic theory predicts [8,9] and computational studies [8] confirm that the diffusion coefficient varies as $D \sim dT^{1/2}$, where d is the particle diameter and T is the granular temperature (velocity variance). In liquidlike rapid, dense flow, experimental [10–13] and computational [3,4] studies indicate $D \sim \dot{\gamma}d^2$, where $\dot{\gamma}$ is the local shear rate. However, in more solidlike quasistatic, or "creep," flow regimes [14,15], where multiple particle contacts exist, particles move collectively, the shear rate is low, and inertia is unimportant, the dependence of D on external excitations (e.g., T or $\dot{\gamma}$) has been less explored.

In this Letter, we computationally study the changes in particle diffusion that occur in granular heap flows between high shear regions found in rapid, dense flow and low shear regions like those in quasistatic creep flow. We find a consistent transitional behavior for diffusion in two distinct flow geometries and over a wide range of velocities, particle size distributions, and mass flow rates. At larger $\dot{\gamma}$, $D \sim \dot{\gamma}d^2$ as in previous studies focusing on the rapid dense flow regime [3,4,11–13]. However, we observe that D is independent of $\dot{\gamma}$ deeper in the bed where shear rates are small. Similar transitions in the shear-rate dependence at similar $\dot{\gamma}$ also occur for the solids fraction and velocity fluctuations. Thus, the transition in D identified here may define the boundary between particle transport driven by shear induced rearrangements and relative motion driven by vibrational fluctuations in elastic contacts.

We used the discrete element method (DEM) to simulate quasi-two-dimensional (quasi-2D) heap flow in two different geometries, a closed heap with a bounding end wall [Fig. 1(a)] and an open heap without a bounding end wall [Fig. 1(b)]. In our quasi-2D heap flow simulations, particles fall onto the heap between two parallel walls with a gap of $B = 1.27$ cm between them and then flow downward via a thin flowing layer at the free surface. To compute the interactions between grains, we used a linear spring-dashpot force model for normal forces and a linear spring model with Coulomb friction for tangential forces when two particles are in contact or overlap with each other. Details and experimental validation of the DEM model appear in Ref. [16]. For these simulations, particles were mm-sized with material density $\rho_p = 2500$ kg/m^3 and a restitution coefficient of 0.8. Particle-particle and particle-wall friction coefficients were 0.4. The binary collision time $t_c = 1 \times 10^{-3}$ s for the majority of our results is consistent with previous simulations [4,16,17] and sufficient for modeling hard spheres in the dense flow regime [18]. Here, t_c is related to particle stiffness, i.e., $t_c \sim \sqrt{m/k}$, where m and k denote particle mass and stiffness, respectively [19]. We separately varied t_c from 1×10^{-4} s to 2×10^{-3} s to investigate the effects of particle stiffness. An integration time step of $\Delta t = t_c/40$ assured numerical stability independent of t_c. We investigated both monodisperse and bidisperse particle size distributions. To reduce particle ordering, particles diameters were uniformly distributed between $0.9d_i$ and $1.1d_i$, where d_i is the mean particle diameter of species i.

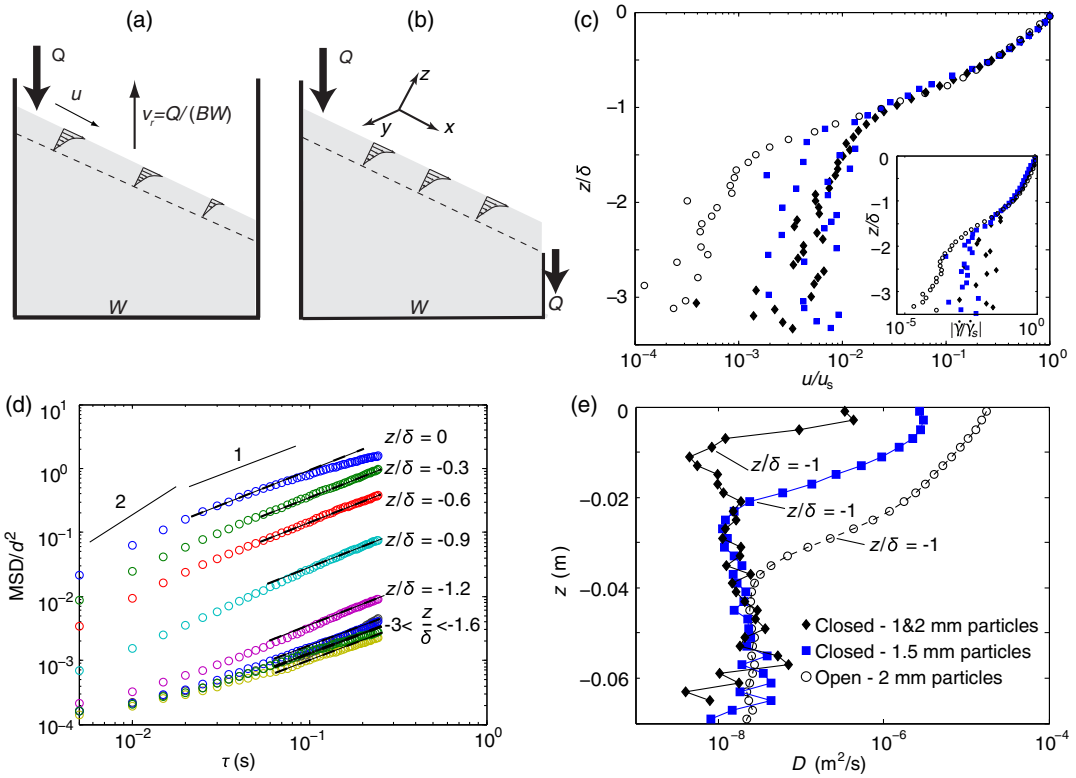

FIG. 1 (color online). (a),(b) Sketch of quasi-2D heaps with (a) closed end wall and (b) open end wall. (c) Normalized streamwise velocity profiles in the depth direction at $x = W/2$ and averaged over the y direction for three simulations: 1.5 mm monodisperse particles at $Q = 60$ cm^3/s (filled squares), 1 and 2 mm bidisperse particles at $Q = 20$ cm^3/s (filled diamonds) in the closed heap, and 2 mm monodisperse particles at $Q = 73$ cm^3/s in the open heap (open circles). Inset: Depth profiles of normalized shear rate $\dot{\gamma}/\dot{\gamma}_s$, where $\dot{\gamma}_s$ is shear rate at the free surface. (d) MSD/d^2 (see text) vs τ at different depths at $x = W/2$ for 2 mm particles at $Q = 73$ cm^3/s in the open heap. Dashed lines indicate a linear fit to the region of each data set where particle motion is diffusive. (e) Diffusion coefficient D vs z at $x = W/2$ for the same conditions as in (c). Data points corresponding to the lower boundary of the flowing layer are labeled as $z/\delta = -1$; $t_c = 1 \times 10^{-3}$ s.

In the closed system [Fig. 1(a)], the heap surface rises at a constant velocity $v_r = Q/BW$, after the heap reaches the downstream bounding end wall. Here, $W = 45.7$ cm is the heap width, and Q is the volumetric feed rate. Due to deposition of particles into the heap, the velocity of particles in the flowing layer varies in both the streamwise (x) and normal (z) directions, and the flowing layer thickness δ decreases slightly in the x direction [16]. We define δ as the depth where the streamwise velocity is equal to 5% of the surface velocity u_s. In the open system [Fig. 1(b)], particles exit the heap at the downstream end. For a sufficiently long heap, the flow is fully developed so that the streamwise velocity u and δ remain constant in the x direction [20]. In steady flow, the two systems share a universal streamwise profile in the z direction in the flowing layer [Fig. 1(c)]. The streamwise velocity decreases rapidly and monotonically from the maximum at the free surface. The shear rate $\dot{\gamma} = |du/dz|$ [inset of Fig. 1(c)] also decreases with increasing depth, but changes most rapidly for $-2 \le z/\delta \le -1$.

We consider diffusion in the z direction only, since particles in heap flow exhibit superdiffusive motion in the streamwise direction due to Taylor dispersion [12,21,22]. The time evolution of the nonaffine component of the z trajectory was calculated using the mean squared displacement (MSD) in the presence of mean flow $\langle \Delta Z(\tau)^2 \rangle$, where $\Delta Z(\tau) = z(t_0 + \tau) - z(t_0) - \Delta L(\tau)$ for each particle [21,23]. Here, $\Delta L(\tau)$ is the mean cumulative displacement of particles in each averaging region (bin) due to mean flow in the z direction at $t_0 + \tau$ for the closed heap, where t_0 is the initial time and τ is the time interval over which the MSD is calculated. The quasi-2D heap was virtually divided into nonoverlapping bins of size $\Delta x = 1$ cm and $\Delta z = 0.2$ cm for the analysis. The angled brackets denote the average for all particles in a bin for 100 values of t_0 with increments of 0.25 s in t_0 after the flow reaches the steady state.

Figure 1(d) shows the MSD vs τ at different depths for an open heap of $d = 2$ mm particles. Similar trends occur for the closed and bidisperse systems. Near the surface ($z/\delta \ge -1.2$), particle motion is ballistic (slope of 2) at smaller time intervals and diffusive (slope of 1) at larger time intervals, similar to slowly sheared, fluidized, dense flow [24]. Further below the flowing layer (more negative values of z), only diffusive motion occurs for the time resolution used here [lower bound of τ in Fig. 1(d)]. D at each depth is based on $\langle \Delta Z^2 \rangle = 2D\tau$ [12] and determined

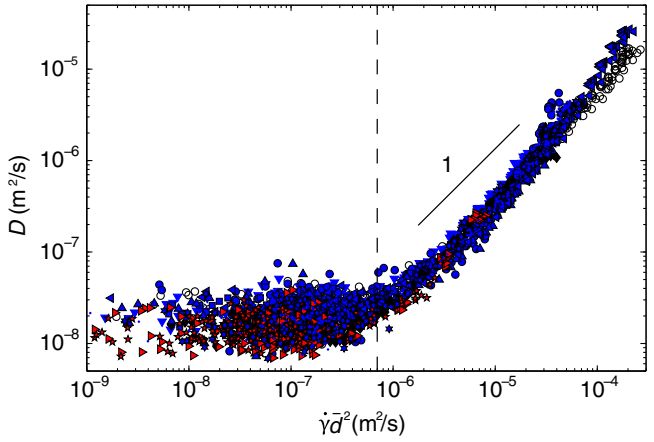

FIG. 2 (color online). Diffusion coefficient D vs $\dot{\gamma}\bar{d}^2$ for the 11 DEM simulations described in Table I. Data for each simulation span the entire length ($0 < x < W$) and depth ($-5\delta < z < 0$) of the heap flow. The dashed line marks the approximate transition ($\dot{\gamma}\bar{d}^2 = 6 \times 10^{-7}$ m^2/s) between shear-rate-dependent and shear-rate-independent diffusion; $t_c = 1 \times 10^{-3}$ s.

by fitting the linear portion (slope of 1) of the MSD profiles in Fig. 1(d). Figure 1(e) shows the depth dependence of D at $x = W/2$ for three simulations: bidisperse particles in the open system and monodisperse particles in the open and closed systems. In all cases, D decreases rapidly from the maximum value at the free surface to a noisy but nearly constant mean value below a certain depth. Even though particle sizes, feed rates, and geometry are different in the simulations, D eventually reaches approximately the same constant value. However, the depth at which the transition to the constant value occurs differs between simulations with varying parameters, and the transitional depth does not always coincide with the arbitrary lower boundary of the flowing layer (data points indicated as $z/\delta = -1$) based on the streamwise velocity profile, most notably for monodisperse grains in the open heap.

Dimensional analysis for dense rapid flow indicates that the time and length scales determining D are $1/\dot{\gamma}$ and the particle size, respectively [11]. Therefore, we plot D vs $\dot{\gamma}\bar{d}^2$ in Fig. 2 for 11 different DEM simulations (Table I), where $\bar{d}$ is the local mean particle diameter for the bidisperse mixture [4]. This scaling collapses all data for a wide range of size distributions, feed rates, and both flow geometries onto the same curve. At larger $\dot{\gamma}\bar{d}^2$, D is proportional to $\dot{\gamma}\bar{d}^2$, consistent with previous studies for rapid, dense flows [3,4,11,12]. However, below a critical $\dot{\gamma}\bar{d}^2$, D is nearly constant. Longer duration simulations in the open heap (not shown) indicate that the observed diffusive scaling in the shear-rate-independent regime persists for MSD values exceeding $\bar{d}^2$. Consequently, these fluctuations in position result in macroscopic particle rearrangement.

To better understand the transition between these two regimes of diffusion, we plot the solids volume fraction f and the local mean squared velocity fluctuation correlations in the x and z directions $u'u'$ and $w'w'$, respectively,

TABLE I. Simulation conditions for data shown in Fig. 2.

d_s (mm)	d_l (mm)	End wall	Q (cm^3/s)	Symbol
2		Open	73	○
1.5		Closed	6.7	▼
1.5		Closed	60	■
1.5		Closed	70	•
1	2	Closed	6.7	♦
1	2	Closed	20	▲
1	2	Closed	70	◀
1	3	Closed	20	▶
1	3	Closed	70	⋆
1.5	2.25	Closed	20	✶
1	1.5	Closed	20	·

vs $\dot{\gamma}\bar{d}^2$ in Fig. 3 for 2 mm diameter particles in the open heap. Here $u'u' = \langle\overline{(u-\bar{u})^2}\rangle$ and $w'w' = \langle\overline{(w-\bar{w})^2}\rangle$, where $\bar{*}$ denotes a bin average at each time and the angled brackets denote a time average. Both quantities exhibit trends similar to D. f increases rapidly with decreasing $\dot{\gamma}$ and then increases more slowly until saturating at a value near the random close packed limit for monodisperse spherical particles $f_c \approx 0.634$ [25,26] [Fig. 3(b)]. The velocity fluctuations decrease as $\dot{\gamma}$ decreases, similar to other dense flow geometries [27], but at small enough $\dot{\gamma}$, both velocity fluctuation components are independent of $\dot{\gamma}$ [Fig. 3(c)]. $u'u'$ and $w'w'$ have different values in the flowing layer due to the anisotropic nature of dense granular flow [11,28], but are nearly

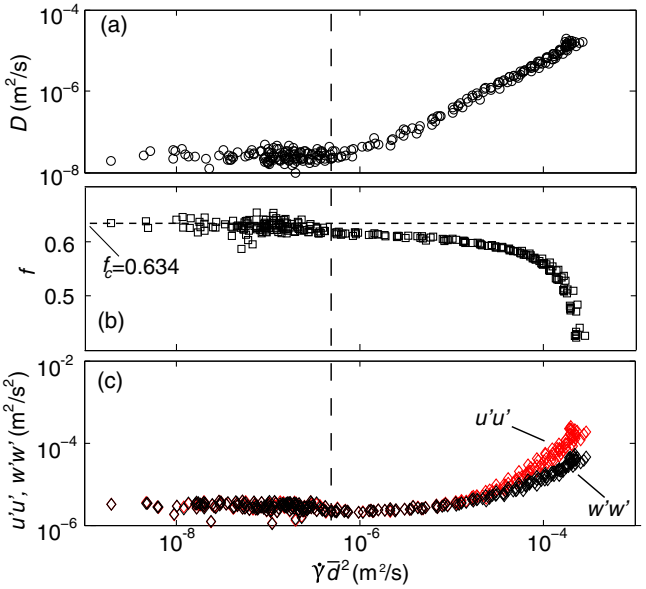

FIG. 3 (color online). Three kinematic properties vs $\dot{\gamma}\bar{d}^2$ for 2 mm particles at $Q = 73$ cm^3/s in the open heap: (a) D, (b) f, and (c) $u'u'$ and $w'w'$. The vertical dashed line indicates the transition shear rate as in Fig. 2. The horizontal dashed line in (b) indicates the random close packed solids fraction for monodisperse spherical particles $f_c = 0.634$ [25,26]; $t_c = 1 \times 10^{-3}$/s.

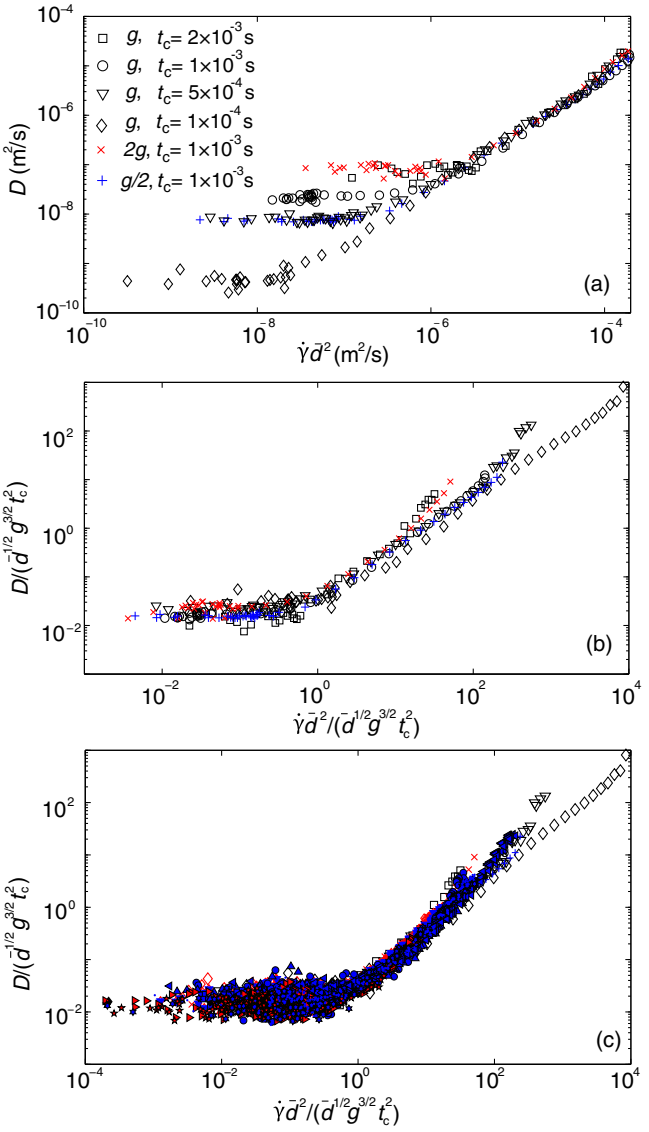

FIG. 4 (color online). (a) D vs $\dot{\gamma}\bar{d}^2$ for three gravitational accelerations and four binary collisional times for 2 mm particles at $Q = 73$ cm^3/s in the open heap. (b) D and $\dot{\gamma}\bar{d}^2$ normalized by $\bar{d}^{1/2}g^{3/2}t_c^2$. (c) D and $\dot{\gamma}\bar{d}^2$ from both Fig. 2 and Fig. 4(a) normalized by $\bar{d}^{1/2}g^{3/2}t_c^2$.

identical at small $\dot{\gamma}$. The qualitative trends in Fig. 3 are independent of flow parameters and simulation parameters, but the transition between regimes varies with t_c and the acceleration due to gravity g, as we discuss next.

In addition to $1/\dot{\gamma}$, dimensional considerations suggest two other relevant time scales: $\sqrt{\bar{d}/g}$ and the binary collision time t_c. Figure 4(a) displays the results of simulations for varying g and t_c for a wide range of $\dot{\gamma}$. At larger shear rates, D for different conditions collapse onto a single curve, indicating that the diffusive motion is not affected by $\sqrt{\bar{d}/g}$ and t_c at larger $\dot{\gamma}$. However, both g and t_c affect the transitional shear rate and the magnitude of D in the shear-rate-independent regime. In this regime, data in Fig. 4(a) collapse when D and $\dot{\gamma}\bar{d}^2$ are scaled by $\bar{d}^{1/2}g^{3/2}t_c^2$, and the transition occurs for $\dot{\gamma}\bar{d}^2/(\bar{d}^{1/2}g^{3/2}t_c^2) = \mathcal{O}(1)$ as shown in Fig. 4(b). The same collapse is observed for different particle sizes, feed rates, flow geometries, gravitational accelerations, and particle collisional times as shown in Fig. 4(c), which combines the data in Fig. 2 with that in Fig. 4(b).

Shear-rate-independent diffusion becomes significant with respect to mixing when particle displacements are on the order of a diameter, i.e., $\sqrt{2Dt}/d > 1$, which corresponds to a "mixing" time $t_m > d^2/(2D)$. From Fig. 4(b), $D \approx 10^{-2}\bar{d}^{1/2}g^{3/2}t_c^2$ so $t_m > 50d^{3/2}g^{-3/2}t_c^{-2}$. For a commonly used granular material such as $d =$ 1 mm glass particles with $t_c = 10^{-5}$ s, $t_m \approx 5 \times 10^5$ s or about six days. However, shear-rate-independent diffusive motion in free surface flows could possibly be observed more readily in softer materials such as rubber ($k_{\text{glass}}/k_{\text{rubber}} \sim 1000$), where t_m would be 500 s or about 10 minutes when the other material parameters remain roughly the same.

The observed scaling is reproduced by considering shear-rate-independent diffusion to be a random walk like elastic contact rearrangement phenomenon driven by oscillations induced by particle collisions in the flowing layer. For a random walk, $D \sim \Delta s^2/\Delta t$, where $\Delta s = F/k$ is the average step size obtained by considering the typical elastic compression of a particle due to the impact of a falling particle and $\Delta t = \sqrt{\bar{d}/g}$ relates the time between steps to the time it takes a particle to fall a distance equal to its diameter. The characteristic collisional force is $F = dp/dt = m\sqrt{\bar{d}g}/t_c$, so $\Delta s \sim t_c\sqrt{\bar{d}g}$. Ignoring constants of $\mathcal{O}(1)$ gives

$$D = \Delta s^2/\Delta t \sim \frac{t_c^2\bar{d}g}{\sqrt{\bar{d}/g}} = \bar{d}^{1/2}g^{3/2}t_c^2,$$

which matches the scaling found in our simulations. The form of the nondimensionalization is consistent with a scaling in simple shear flow wherein the mean pressure is assumed linearly proportional to particle stiffness [29].

The observed scaling in the shear-rate-independent regime is different from the $\mu - I$ rheology [30–32] for inertial flow in which μ is a friction coefficient and $I = \dot{\gamma}\sqrt{d^2\rho_p/P}$ (where P is the pressure) is the inertia number which characterizes the ratio of the inertia time scale to the macroscopic deformation time scale. Recent studies [33,34] emphasize that the $\mu - I$ model is inappropriate to apply in quasistatic creep flow where I is small. In the shear-rate-independent regime, we found that gravity and particle stiffness play important roles in diffusion—different characteristic time scales than used in the $\mu - I$ model [30–32]. Our results provide a different understanding of the quasistatic creep regime which falls outside the scope of the $\mu - I$ rheology and also reveals insights into the mechanics of nonlocal flows proposed in recent models [35,36].

Our simulation results imply the existence of a relatively homogeneous regime in which the solids fraction is constant and diffusion is driven by particles mobilized by force fluctuations in the contact network. These

fluctuations are apparently nonlocal and are presumably driven by collisions of particles in the feed zone and in the flowing layer. This picture is not incompatible with shear-rate-independent particle motion observed in other granular flow experiments, such as particle motion in slowly drained vertical structures [1,37–39]. In these studies, shear is largely absent and fluctuations are driven by the decrease in the gravitational potential energy of any given particle as it descends. In draining experiments, diffusive particle motion was observed in the MSD at times long compared to the ballistic time scale [37] and for fall distances on the order of a particle diameter [1]. Choi *et al.* suggest that in the absence of shear, diffusive motion is the result of random rearrangements of local particle clusters driven by fluctuations in the contact network [1]. Particle motion driven purely by the rearrangement of the contact network in the absence of any flow has also been reported when using thermal cycling to compact particle beds [40].

Although we considered a range of flows and particle sizes and stiffnesses, other flow conditions, such as non-gravity-driven flow (e.g., annular shear flow), should also be examined to clarify the generality of our results. In addition, study of the microstructure using statistical characteristics of the force networks and correlations between particle packing and motion may provide further insights into the motion in the shear-rate-independent transport regime. Last, experimental verification, presumably using soft particles, would be useful in further exploring shear-rate-independent diffusion. Nevertheless, it is clear that shear drives granular diffusion under the high shear-rate conditions typical of rapid, dense flow, while an elastic phenomenon, likely related to excitations translated through force chains, drives diffusion in the underlying bed of particles, which can shed light on the understanding of creep dynamics in both dry granular flow and fluid-granular flow [41,42].

We thank Karl Jacob, Ben Freireich, Ivan Christov, Eric Weeks, and Martin van Hecke for helpful discussions. We gratefully acknowledge financial support from The Dow Chemical Company.

*yfan5@dow.com
†r-lueptow@northwestern.edu

[1] J. Choi, A. Kudrolli, R. R. Rosales, and M. Z. Bazant, Phys. Rev. Lett. **92**, 174301 (2004).
[2] Y. Fan, Y. Boukerkour, T. Blanc, P. B. Umbanhowar, J. M. Ottino, and R. M. Lueptow, Phys. Rev. E **86**, 051305 (2012).
[3] A. Tripathi and D. Khakhar, J. Fluid Mech. **717**, 643 (2013).
[4] Y. Fan, C. P. Schlick, P. B. Umbanhowar, J. M. Ottino, and R. M. Lueptow, J. Fluid Mech. **741**, 252 (2014).
[5] C. P. Schlick, Y. Fan, P. B. Umbanhowar, J. M. Ottino, and R. M. Lueptow, J. Fluid Mech. **765**, 632 (2015).
[6] G. Marty and O. Dauchot, Phys. Rev. Lett. **94**, 015701 (2005).
[7] E. R. Weeks and D. A. Weitz, Phys. Rev. Lett. **89**, 095704 (2002).
[8] S. B. Savage and R. Dai, Mech. Mater. **16**, 225 (1993).
[9] S. Hsiau and M. Hunt, J. Heat Transfer **115**, 541 (1993).
[10] J. Bridgwater, Powder Technol. **25**, 129 (1980).
[11] V. Natarajan, M. Hunt, and E. Taylor, J. Fluid Mech. **304**, 1 (1995).
[12] B. Utter and R. P. Behringer, Phys. Rev. E **69**, 031308 (2004).
[13] H. Katsuragi, A. R. Abate, and D. J. Durian, Soft Matter **6**, 3023 (2010).
[14] T. S. Komatsu, S. Inagaki, N. Nakagawa, and S. Nasuno, Phys. Rev. Lett. **86**, 1757 (2001).
[15] B. A. Socie, P. Umbanhowar, R. M. Lueptow, N. Jain, and J. M. Ottino, Phys. Rev. E **71**, 031304 (2005).
[16] Y. Fan, P. B. Umbanhowar, J. M. Ottino, and R. M. Lueptow, Proc. R. Soc. A **469**, 20130235 (2013).
[17] P. Chen, J. M. Ottino, and R. M. Lueptow, New J. Phys. **13**, 055021 (2011).
[18] L. E. Silbert, G. S. Grest, R. Brewster, and A. J. Levine, Phys. Rev. Lett. **99**, 068002 (2007).
[19] J. Schafer, S. Dippel, and D. E. Wolf, J. Phys. I (France) **6**, 5 (1996).
[20] GDR MiDi, Eur. Phys. J. E **14**, 341 (2004).
[21] E. Wandersman, J. A. Dijksman, and M. van Hecke, Europhys. Lett. **100**, 38006 (2012).
[22] I. Christov and H. Stone, Granular Matter **16**, 509 (2014).
[23] R. Besseling, E. R. Weeks, A. B. Schofield, and W. C. K. Poon, Phys. Rev. Lett. **99**, 028301 (2007).
[24] A. S. Keys, A. R. Abate, S. C. Glotzer, and D. J. Durian, Nat. Phys. **3**, 260 (2007).
[25] R. D. Kamien and A. J. Liu, Phys. Rev. Lett. **99**, 155501 (2007).
[26] C. Song, P. Wang, and H. A. Makse, Nature (London) **453**, 629 (2008).
[27] W. Losert, L. Bocquet, T. C. Lubensky, and J. P. Gollub, Phys. Rev. Lett. **85**, 1428 (2000).
[28] Y. Fan and K. M. Hill, New J. Phys. **13**, 095009 (2011).
[29] S. Chialvo, J. Sun, and S. Sundaresan, Phys. Rev. E **85**, 021305 (2012).
[30] F. da Cruz, S. Emam, M. Prochnow, J.-N. Roux, and F. Chevoir, Phys. Rev. E **72**, 021309 (2005).
[31] P. Jop, Y. Forterre, and O. Pouliquen, Nature (London) **441**, 727 (2006).
[32] Y. Forterre and O. Pouliquen, Annu. Rev. Fluid Mech. **40**, 1 (2008).
[33] P. Jop, Phys. Rev. E **77**, 032301 (2008).
[34] G. Koval, J.-N. Roux, A. Corfdir, and F. Chevoir, Phys. Rev. E **79**, 021306 (2009).
[35] K. Kamrin and G. Koval, Phys. Rev. Lett. **108**, 178301 (2012).
[36] D. L. Henann and K. Kamrin, Proc. Natl. Acad. Sci. U.S.A. **110**, 6730 (2013).
[37] N. Menon and D. J. Durian, Science **275**, 1920 (1997).
[38] S. Moka and P. R. Nott, Phys. Rev. Lett. **95**, 068003 (2005).
[39] J. J. Drozd and C. Denniston, Phys. Rev. E **78**, 041304 (2008).
[40] K. Chen, J. Cole, C. Conger, J. Draskovic, M. Lohr, K. Klein, T. Scheidemantel, and P. Schiffer, Nature (London) **442**, 257 (2006).
[41] V. B. Nguyen, T. Darnige, A. Bruand, and E. Clement, Phys. Rev. Lett. **107**, 138303 (2011).
[42] M. Houssais, C. P. Ortiz, D. J. Durian, and D. J. Jerolmack, Nat. Commun. **6**, 6527 (2015).